TTC-0161
SAND-80-2302
Unlimited Release
Printed February 1981

PHYSICAL AND MECHANICAL PROPERTIES OF CAST 17-4 PH STAINLESS STEEL*

H. J. Rack
Mechanical Metallurgy Division 5835
Sandia National Laboratories,† Albuquerque, New Mexico 87185

ABSTRACT

The physical and mechanical properties of an overaged 17-4 PH stainless steel casting have been examined. The tensile and compressive properties of cast 17-4 PH are only influenced to a slight degree by changing test temperature and strain rate. However, both the Charpy impact energy and dynamic fracture toughness exhibit a tough-to-brittle transition with decreasing temperature--this transition being related to a change in fracture mode from ductile, dimple to cleavage-like. Finally, although the overaged 17-4 PH casting had a relatively low room temperature Charpy impact energy when compared to wrought 17-4 PH, its fracture toughness was at least comparable to that of wrought 17-4 PH. This observation suggests that prior correlations between Charpy impact energies and fracture toughness, as derived from wrought materials, must be approached with caution when applied to cast alloys.

*This work sponsored by the U. S. Department of Energy under Contract DE-AC04-76-DP00789.

†A U. S. Department of Energy facility.

ACKNOWLEDGMENT

The author wishes to acknowledge the assistance of [illegible]. C. Powe, R. Blose and M. Sturm in the mechanical testing and scanning electron microscopy portions of this program.

CONTENTS

This Page Intentionally Left Blank.

INTRODUCTION

Prior studies of 17-4 PH stainless steel (1-11) have generally considered the mechanical and physical properties of wrought product forms, that is rolled plate, forgings, etc. There are, however, many instances where, because of economic considerations, 17-4 PH stainless steel castings might be an attractive alternative. Unfortunately, little information exists on the mechanical and physical properties of 17-4 PH stainless steel castings. This report presents the results of an evaluation of such a casting. Where available, direct comparison with data obtained from wrought 17-4 PH stainless steel is also included.

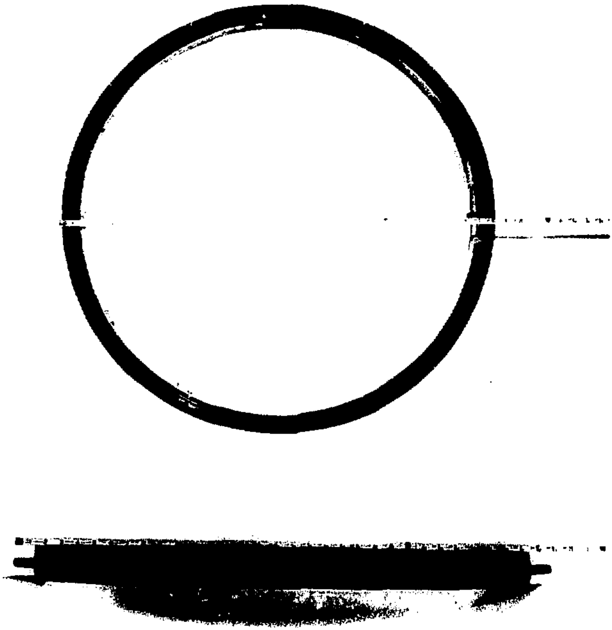

Figure 1. Top and Side Views of 17-4 PH Stainless Steel Seal Casting.

EXPERIMENTAL PROCEDURE

Figure 1 shows the 17-4 PH stainless steel casting evaluated in this study. This casting was selected since it is currently being considered as the primary metallic seal for a liquid metal breeder reactor spent fuel shipping container. As such, the seal must operate at temperatures between 233 and 473K. In addition, it must be able to withstand applied strain rates approaching 10 sec^{-1}.

Physical Properties

Physical property measurements of the 17-4 PH stainless steel casting involved determinations of the linear expansion, specific heat and thermal diffusivity as a function of temperature. A dual fused silica pushrod Theta dilatometer* operating in a room temperature environment was used to obtain linear expansion measurements in the temperature range 298 to 1173K (12). Measurements between 298 to 213K were made with a single fused silica pushrod dilatometer, again maintained in a room temperature environment. Finally, the linear expansion samples, 25.4 mm in length x 2.54 mm square, were equilibrated for one hour at each test temperature prior to expansion measurements.

Specific heat determinations utilized a Perkin Elmer Model DSC-2 differential scanning calorimeter connected to a PDP minicomputer-based digital data acquisition system (13). The thermal diffusivity results were obtained using a computer controlled laser flash diffusivity technique (13). Knowing the specific heat, C_p, and the thermal diffusivity α, the thermal conductivity, , was then calculated from

(1)

where is the density corrected for changes in temperature relative to room temperature (298K).

---

*The dilatometer was calibrated using standard fused silica and platinum samples.

Mechanical Behavior

The elastic properties of the 17-4 PH stainless steel casting were measured over the temperature range 233 to [illegible]K using standard ultrasonic techniques (14). These techniques require that the travel time, t, for an ultrasonic wave to propagate through a known specimen length, [illegible], be obtained as a function of temperature. Once this travel time is [illegible], the ultrasonic velocity, V, can be determined from

[illegible]

[illegible]

[illegible]

$$E = 2 [illegible]$$

[illegible]

[illegible] are the shear modulus, Young's modulus, [illegible] [illegible], respectively. [illegible], the latter [illegible] [illegible] increasing/decreasing temperature about 298K.

The elastic behavior of the 17-4 PH stainless steel casting was [illegible] using standard tensile, compression and Charpy [illegible] (precracked) test procedures. Figure 2 illustrates the [illegible] of these samples as removed from the 17-4 PH stainless steel [illegible] casting.* Tensile and compression tests were performed between strain rates of 1.3 x [illegible] and 1.2 sec^{-1} over a temperature range 215 [illegible] [illegible]5K.

---

*The actual sample configurations are given in more detail in Appendix [illegible].

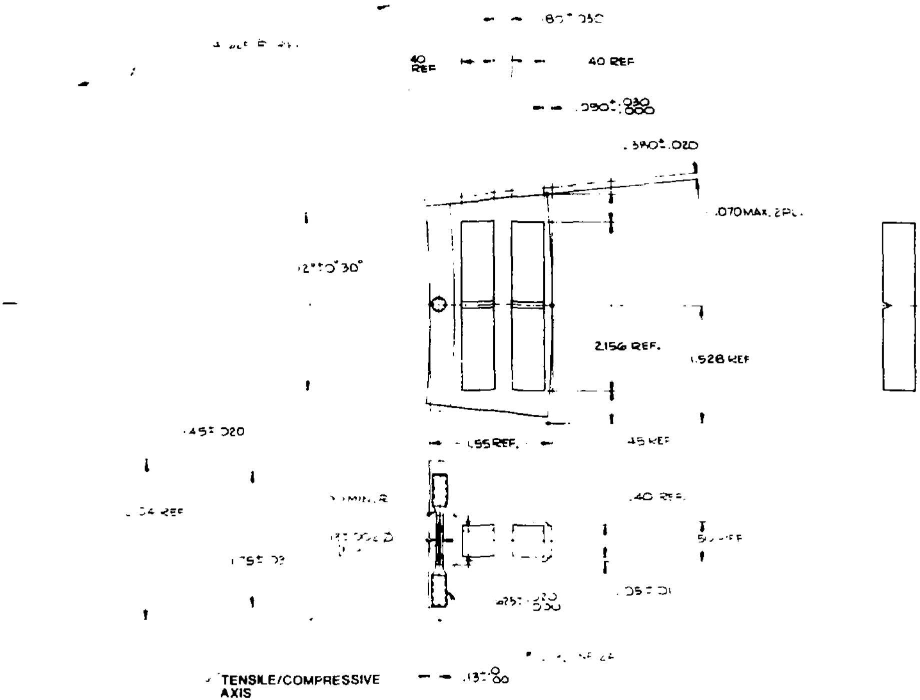

Figure 2. [illegible] 17-4 [illegible] 2.54 cm).

The Charpy impact samples were tested in either the V-notched or fatigue precracked condition. Fatigue precracking utilized methods [15] where the final stress intensity during precracking, K_{f}, was always [illegible] at less than one-half of the dynamic fracture toughness, K_{Id}. Both the notched and fatigue precracked samples were tested using [illegible] instrumented impact machine with the initial impact velocity being [illegible] (16,17).

[illegible] fracture was elastic, that is, no general yielding was [illegible], the fracture toughness, K_{Id}, was obtained from the precracked [illegible] calculated from [illegible]:

$$K_{Id} = \frac{4P_{M}}{BW^{1/2}} \left[[\text{illegible}] \left(\frac{a}{W}\right)^{1/2} - [\text{illegible}] \left(\frac{a}{W}\right)^{3/2} + [\text{illegible}] \left(\frac{a}{W}\right)^{5/2} \right.$$

$$\left. - [\text{illegible}] \left(\frac{a}{W}\right)^{7/2} + [\text{illegible}]8.[\text{illegible}] \left(\frac{a}{W}\right)^{9/2} \right] \qquad (5)$$

[illegible] maximum load, [illegible] the crack [illegible] yielding was observed, i.e., at [illegible] test temperature [illegible] of the fracture toughness was obtained from [illegible] the [illegible] value of the J integral, i.e.,

$$K_{JD} = (EJ_{Id})^{1/2} \qquad (6)$$

[illegible]

$$J_{Id} = 2E_{M}/Bb \qquad (7)$$

[illegible] and E_{M} was taken as the true specimen energy to [illegible] load (18).

RESULTS AND DISCUSSION

General

The chemical composition of the 17-4 PH stainless steel casting examined in this study is given in Table 1. Before machining, this casting had been homogenized at 1422K and then solution treated at 1311K. Final aging involved a four hour exposure at 922K. Optical microscopy indicated that the casting possessed an aged α-martensite matrix with δ-ferrite stringers, Figure 3. High magnification examination of the α-martensite matrix, Figure 4, indicated that the casting was in the overaged heat treatment condition; that it contained a rather coarse dispersion of the primary strengthening phase, spherical face centered cubic Cu particles. Further examination, Figure 5, revealed the presence of rod-shaped precipitates within the δ-ferrite stringers. X-ray energy dispersive analysis, Figure 6, indicated that these particles were relatively rich in Cu when compared to the δ-ferrite matrix. The appearance of these rod-shaped Cu rich particles within the δ-ferrite stringers seems to be restricted to 17-4 PH stainless steel castings since their presence has not been reported in previous studies of wrought 17-4 PH stainless steel (1-11).

Table 1

Chemical Composition of 17-4 PH Casting

Element	Weight Percent
Cr	16.94
Ni	4.0
Cu	3.0
Mn	0.5
C	0.044
S	0.022
Si	0.7
Nb	0.3
Fe	Bal.

Figure 3. Optical Micrograph of 17-4 PH Stainless Steel Casting. White Areas δ-Ferrite Stringers; Darker Matrix Aged α-Martensite. Original Magnification 100X.

Figure 4. Transmission Electron Micrograph of Aged α-Martensite in 17-4 PH Stainless Steel Casting Containing Spherical Cu Precipitates. Original Magnification: 40,000X.

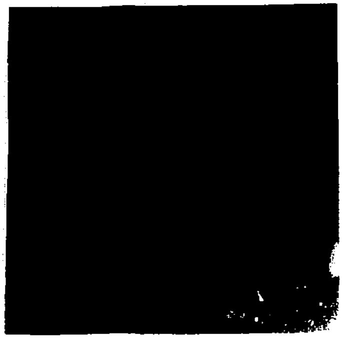

Figure 5. Transmission Electron Micrograph of δ-Ferrite Stringer Containing Rod-Shaped Cu-Rich Precipitate. Original Magnification: 52,000X.

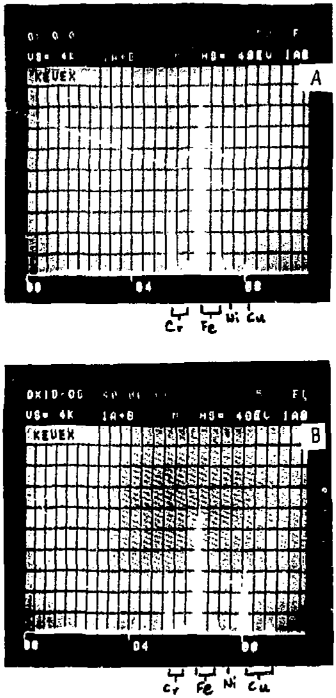

Figure 6. X-Ray Energy Dispersive Spectra From (a) δ-Ferrite Matrix and (b) Rod-Shaped Particles Shown in Fig. 5.

[illegible]

The results [illegible] measurements are tabulated [illegible] 2 and plotted [illegible]. This figure shows that the [illegible] [illegible] latter [illegible] dashed line [illegible]

[illegible] agreement between the properties of wrought and cast 17-4 [illegible] steel was not observed [illegible] properties [illegible]. The results of the [illegible] heat and thermal [illegible] measurements are tabulated in Tables [illegible] and 4, respectively, [illegible] calculated values of the thermal [illegible] presented in Table 5. This tabulated data is plotted in Figures [illegible] and 10, with the dashed lines in Figures 8 and 10 [illegible] of previous data [illegible] wrought 17-4 PH stainless steel [illegible]. In general, these results indicate that the thermal properties [illegible] 17-4 PH stainless steel appear to [illegible] in temperature than would be expected from the wrought [illegible] stainless steel data. [illegible] 17-4 PH [illegible] two products may be [illegible] increased [illegible]

Table 2

Thermal Linear Expansion of 17-4 PH
Stainless Steel Casting

Temperature (F)	$\Delta L/L_o$ (Pct.)
279	-0.020
298	0.000
474	0.194
476	0.199
568	0.313
626	0.373
627	0.372
643	0.409
775	0.546
781	0.562
783	0.566
917	0.711
919	0.671
925	0.703
1064	0.824
1212	1.107

Table 3

Specific Heat of 17-4 PH Stainless Steel Casting

Temperature (K)	Specific Heat (W sec gm^{-1} K^{-1})
350	0.4750
375	0.4884
400	0.4973
425	0.5054
450	0.5147
460	0.5220
475	0.5228
500	0.5335
525	0.5396
550	0.5477
575	0.5548
600	0.5636
625	0.5726
650	0.5805
675	0.5885
700	0.5978
725	0.6080
750	0.6341
775	0.6594
795	0.6812
800	0.6875
825	0.724[illegible]
850	0.7409
875	0.7576
900	0.7672
925	0.778[illegible]

Table 4

Thermal Diffusivity of 17-4 PH Stainless Steel Casting

Temperature (K)	Diffusivity (cm^2 sec^{-1})
294	0.0458
461	0.0452
627	0.0457
794	0.0430
961	0.0475
1127	0.0548

Table 5

Thermal Conductivity of 17-4 PH Stainless Steel Casting

Temperature (K)	Conductivity (W cm^{-1} K^{-1})
294	0.152
461	0.180
627	0.199
794	0.206
961	0.281

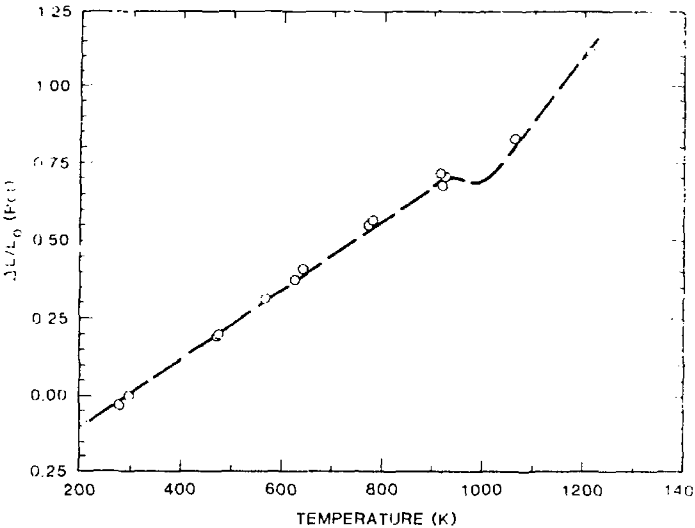

Figure [illegible]. Linear Thermal Expansion of 17-4 PH Stainless Steel. Data Points from 17-4 PH Casting, Dashed Line an [illegible] 17-4 PH Steel [illegible] Steel [illegible]

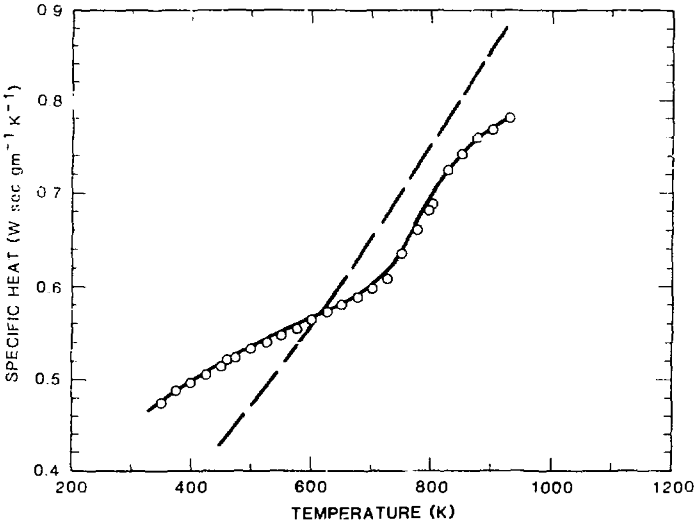

Figure 8. Specific Heat of 17-4 PH Stainless Steel as a Function of Temperature. Data Points from 17-4 PH Casting, Dashed Line an Average Obtained from Wrought 17-4 PH Stainless Steel (21).

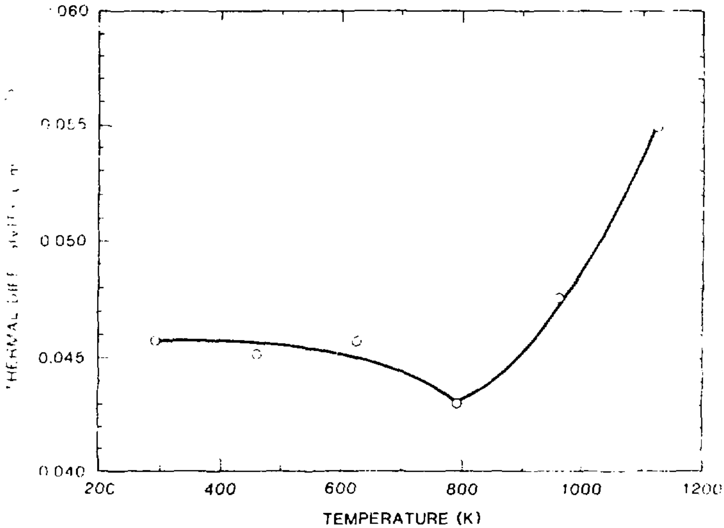

Fig. [illegible]. Thermal Diffusivity of Cast 17-4 PH Stainless Steel as a Function of Temperature.

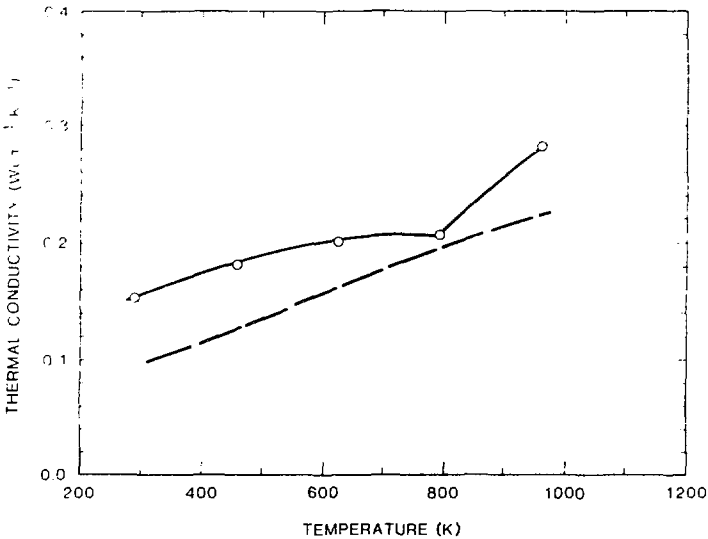

Figure 10. Thermal Conductivity of 17-4 PH Stainless Steel as a Function of Temperature. Data Points from 17-4 PH Casting, Dashed Line an Average Obtained from Wrought 17-4 PH Stainless Steel (2).

Table 6

Young's Modulus and Poisson's Ratio
of 17-4 PH Casting

Temperature (K)	Young's Modulus (GPa)	Poisson's Ratio
248	211.0	0.283
297	204.2	0.291
298	204.1	0.291
301	202.8	0.288
494	194.6	0.295
501	191.5	0.296
580	186.7	0.296
582	186.2	0.294
650	182.2	0.306
650	181.9	0.304
728	176.3	0.316
742	174.0	0.307
798	167.8	0.309
817	164.7	0.321
885	153.3	0.322
957	142.3	0.332
1031	134.0	0.344
1067	128.8	0.348
1151	118.0	0.359
1162	117.3	0.361

Shear Mod[illegible]

[illegible]	Shear [illegible]
249	82.[illegible]
2[illegible]	[illegible]
[illegible]	[illegible]
[illegible]2	[illegible]
4[illegible]	[illegible]
5[illegible]	[illegible]
56[illegible]	[illegible]
[illegible]	[illegible]
[illegible]	[illegible]
6[illegible]5	[illegible]
[illegible]	[illegible]
[illegible]4[illegible]	[illegible]5.[illegible]
[illegible]	[illegible]
[illegible]	[illegible]
[illegible]	[illegible]
[illegible]	[illegible]
[illegible]85	[illegible]
[illegible]	[illegible]
[illegible]	[illegible]
[illegible]	[illegible]
[illegible]	[illegible]

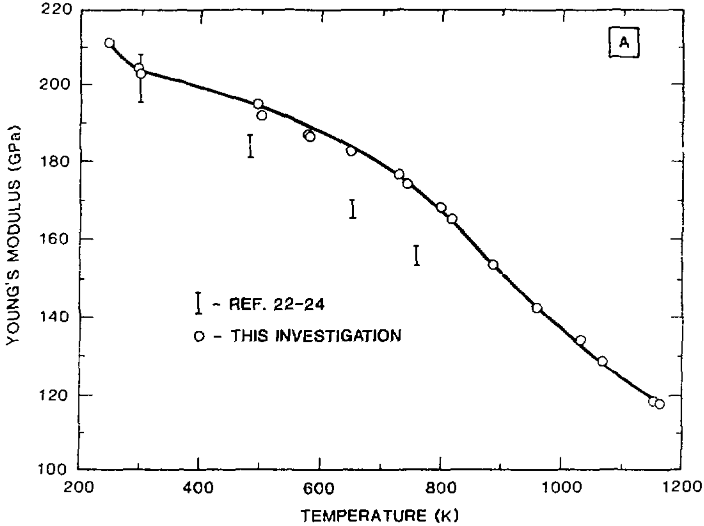

Figure 11. Elastic Properties of Overaged 17-4 PH Stainless Steel Casting (a) Young's Modulus, (b) Shear Modulus and (c) Poisson's Ratio.

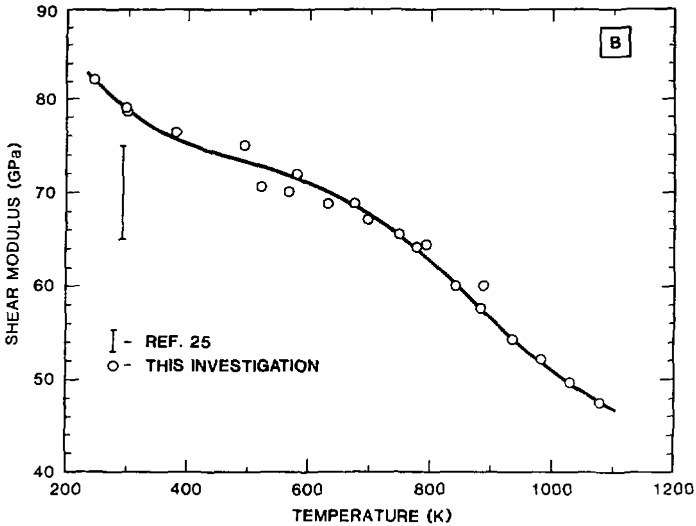

Figure 11. (Cont'd)

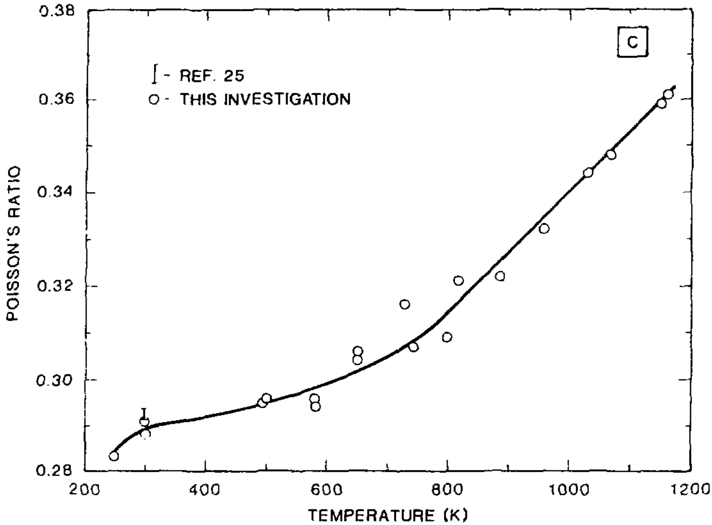

Figure 11. (Cont'd)

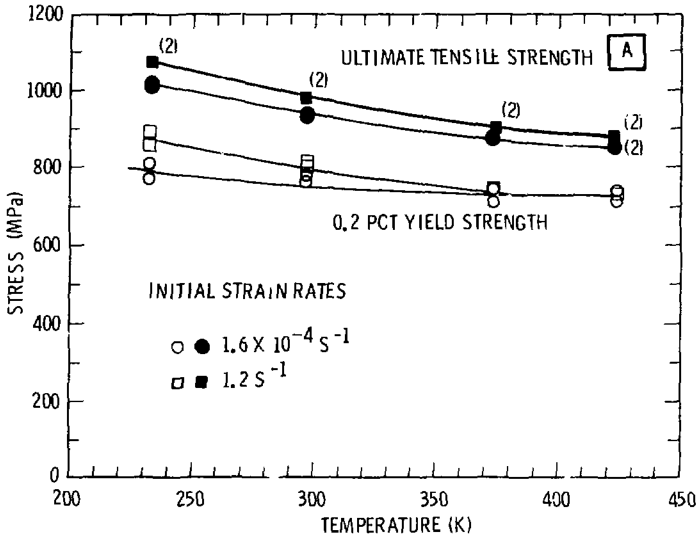

Figure 12. Influence of Test Temperature and Strain Rate on the Tensile Properties of Overaged Cast 17-4 PH Stainless Steel.

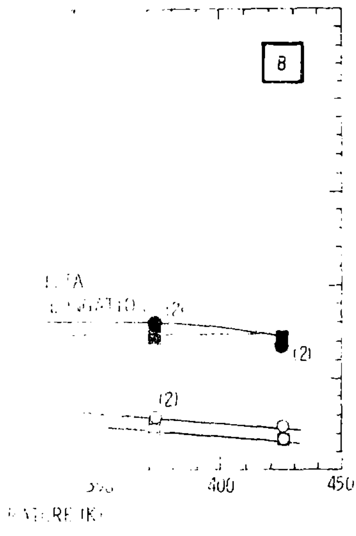

B
(2)
(2)
(2)
400
450

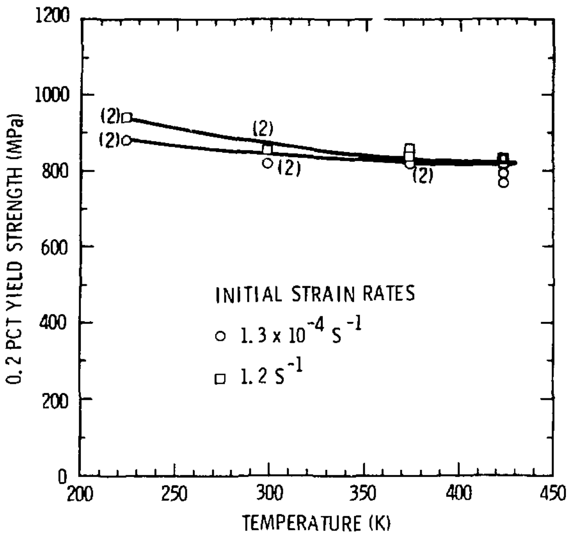

Figure 13. Influence of Test Temperature and Strain Rate on Compressive Yield Strength of Overaged Cast 17-4 PH Stainless Steel.

temperature and strain rate. Figure 12(b) shows that the uniform elongation decreased with both increasing test temperature and strain rate. This figure further indicates that, except at the lowest strain [illegible] 1.0 x 10^{-4} s^{-1}, and the highest test temperature, 433K, the [illegible] elongation was independent of test temperature and decreased [illegible] increasing strain rate. Finally, fractographic examination showed [illegible] tensile failure mode was, in all cases, characterized by the [illegible] of transgranular dimples, with the larger dimples being [illegible] ated with various inclusions and δ-ferrite, Figure 14.

[illegible] assically, the fracture toughness behavior of low strength [illegible] alloys has been examined by considering the influence of test [illegible] ture on the energy absorbed during impa[illegible] fracture of a standar[illegible] [illegible] notch specimen. These investigations have typically shown [illegible] these steels undergo a tough-to-brittle transition with decreasing [illegible] ture, that is, there is a large reduction in absorbed energy [illegible] relatively small temperature region. Figure 15 shows that the [illegible] pact energy of the overaged 17-4 PH stainless steel casting [illegible] under study also underwent such an energy related transition, [illegible] both the values of the upper shelf energy and rate of energy [illegible] with decreasing temperature were less than those normally [illegible] r lower strength alloys (26). If a typical 20 joule absorbed [illegible] tough-to-brittle transition temperature criteria were applied to [illegible] cast 17-4 PH, the T_{25J} transition temperature would have been [illegible] 356K, i.e., well above room temperature. Finally, com[illegible] of the room temperature Charpy impact energy obtained for the [illegible] cast 17-4 PH (E ~ 11 joules) with that reported for wrought 17-4 PH [illegible] at 866K (7) (E ~ 37 joules) suggests that cast 17-4 PH will absorb two-thirds less energy during impact loading than will wrought 17-4 PH.

Although the dynamic fracture toughness measurements--as shown in Figure 16--also exhibited such a tough-to-brittle transition behavior,

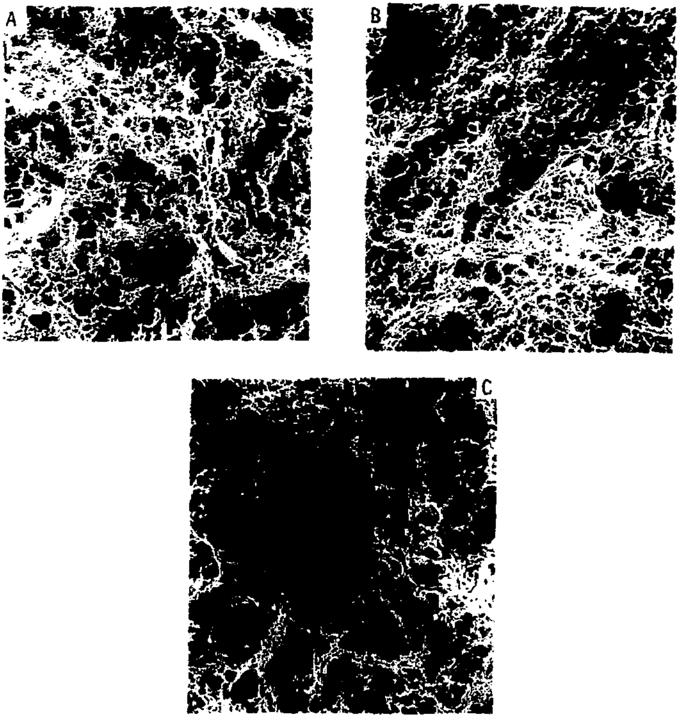

Figure 14. Scanning Electron Fractographs of Cast 17-4 PH Stainless Steel Tensile Samples Tested at:

(a) $\dot{\varepsilon} = 1.6 \times 10^{-4}\ s^{-1}$, $T = 233K$;

(b) $\dot{\varepsilon} = 1.6 \times 10^{-4}\ s^{-1}$, $T = 423K$; and

(c) $\dot{\varepsilon} = 1.2\ s^{-1}$, $T = 423K$.

Original Magnification: 400X.

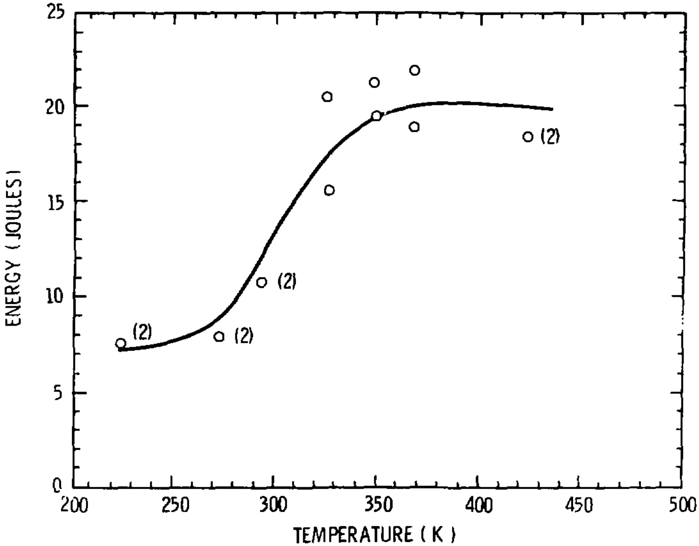

Figure 15. Charpy Impact Energy-Temperature Relationship in Cast 17-4 PH Stainless Steel.

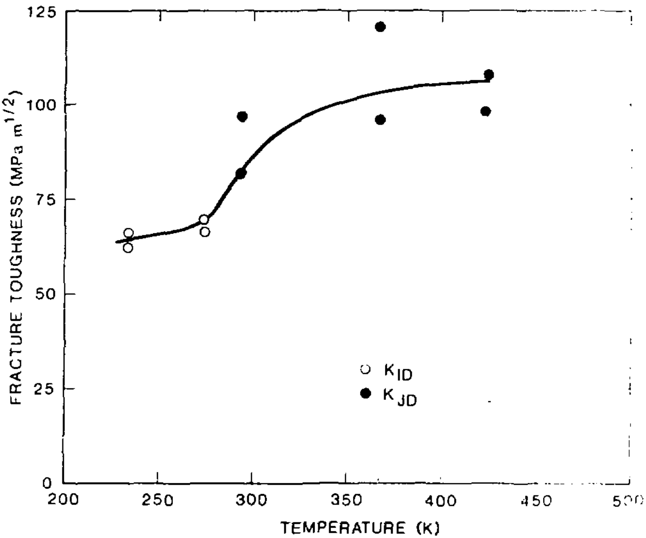

Figure 16. Dynamic Fracture Toughness-Temper[illegible]
Cast 17-4 PH Stainless Steel.

the fracture toughness of the overaged 17-4 PH casting, even at the lowest test temperature examined, was still quite high, approximately 60 $MPam^{1/2}$. In addition, the room temperature toughness ($\sim$ 90 $MPam^{1/2}$) was at least comparable to that observed in wrought, overaged 17-4 PH (27), K_{IC} $\sim$ 130 $MPam^{1/2}$. These observations reinforce those of Floreen (28), wherein he concluded that Charpy impact energy-fracture toughness correlations previously suggested for wrought products are generally <u>not</u> applicable to castings, that is, the latter's Charpy impact values are typically quite low, even though their fracture toughness properties may be high.

Finally, fractographic examination of the Charpy V-notch and precracked samples indicated that the fracture toughness transitions described above could be related to a change in fracture mode. At temperatures above 350K, failure in both types of samples involved microvoid initiation and growth, Figure 17(a). Decreasing the test temperature below 350K resulted in the introduction of increasing amounts of cleavage-like failure, Figure 17(b).

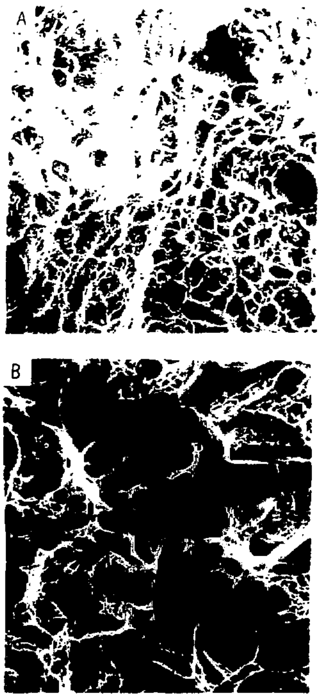
A
B

This Page Intentionally Left Blank.

SUMMARY AND CONCLUSIONS

This investigation has examined the physical and mechanical [illegible] of an overaged 17-4 PH stainless steel casting and has [illegible] these properties, where available, with those for wrought 17-4 PH stainless steel. The study has shown that--

1. The linear expansion behavior of cast 17-4 PH is identical to that of the wrought alloy.

2. The thermal properties, specific heat, thermal diffusivity and thermal conductivity, of cast 17-4 PH stainless steel are more sensitive to temperature than is wrought 17-4 PH, that is, they vary in a more complicated fashion with temperature than do the thermal properties of wrought 17-4 PH.

3. The elastic properties, Young's modulus and shear modulus, tend to be higher in cast 17-4 PH stainless steel than in the wrought alloy, although they [illegible] decrease with increasing temperature.

4. The tensile and compressive properties of cast 17-4 PH were to some degree a function of test temperature and strain rate, although not to the same degree as for lower strength ferrous steels.

5. The Charpy V-notch impact energy and the dynamic fracture toughness both exhibited a tough-to-brittle transition with decreasing test temperature. This transition was related to a change in [illegible] ductile, dimple to [illegible].

6. [illegible] Charpy impact energy for cast 17-4 PH [illegible] one-third that of wrought 17-4 PH, [illegible] fracture toughness of cast and wrought 17-4 PH were comparable. This reinforces [illegible] suggestions that Charpy impact-fracture toughness correlations obtained for wrought [illegible] may not be applicable to castings.

REFERENCES

1. K. C. Antony, Aging Reactions in Precipitation Hardenable Stainless Steel, J. Metals, 15, 922 (1963).

2. E. Hornbogen and R. C. Glenn, A Metallographic Study of Precipitation of Cu from α Fe, Trans. Met. Soc. AIME, 218, 1064 (1960).

3. E. Hornbogen, Aging and Plastic Deformation of a Fe-0.9% Cu Alloy, Trans. ASM, 57, 120 (1964).

4. E. Hornbogen, The Role of Strain Energy During Precipitation of Cu and Au from α-Fe, Acta Met., 10, 525 (1962).

5. K. C. Russell and L. M. Brown, A Dispersion Strengthening Model Based on Differing Elastic Moduli Applied to the Fe-Cu System, Acta Met., 20, 969 (1972).

6. A. Youle and B. Ralph, A Study of the Precipitation of Cu from α-Fe in the Pre-Peak to Peak Hardness Range of Aging, Met. Sci. Jn., 6, 149 (1972).

7. H. J. Rack and David Kalish, The Strength, Fracture Toughness and Low Cycle Fatigue Behavior of 17-4 PH Stainless Steel, Met. Trans., 5, 1595 (1974).

8. G. N. Goller and N. C. Clarke, Jr., New Precipitation-Hardening Stainless Steels, Iron Age, 165, 86 (1950).

9. K. J. Irvine, D. T. Llewellyn and F. B. Pickering, Controlled-Transformation Stainless Steels, J. Iron Steel Inst., 192, 218 (1959).

10. C. S. Carter, D. G. Farwick, A. M. Ron and J. M. Ucheda, Stress Corrosion Properties of High Strength, Precipitation Hardening Stainless Steel, Corrosion, 27, 190 (1971).

11. E. A. Lauchner, The Microstructure and Ductility of 17-4 PH and 15-5 PH Stainless Steels, J. Material, 5, 129 (1970).

12. Memo, J. E. McCreight to H. J. Rack, November 28, 1979, subject: Thermal Expansion Measurements.

13. R. E. Taylor and H. Groot, Thermophysical Properties of Alloys, TPRL 195, Thermophysical Properties Research Laboratory, Purdue University, West Lafayette, Indiana, August 1979.

14. J. F. Gieske, Ultrasonic Measurement of Elastic Moduli of 17-4 PH Stainless Steel and U-2 wt. pt M_o from -40° to 800°C, SAND80-1121, July 1980.

15. J. M. Krafft and R. A. Gray, "Effects of Neutron Irradiation on Bulk and Micro Flow-Fracture Behavior of Pressure Vessel Steels," in Practical Applications of Fracture Mechanics to Pressure Vessel Technology, Institution of Mechanical Engineers, London, 1971, pp. 93-102.

16. R. A. Wullaert, Applications of the Instrumented Charpy Impact Test, Impact Testing of Metals ASTM STP 466, Am. Soc. Testing and Materials, Philadelphia, PA, 1970, pp. 148-164.

17. W. L. Server and A. S. Tetelman, The Use of Pre-Cracked Charpy Specimens to Determine Dynamic Fracture Toughness, Eng. Fract. Mech., 4, 367 (1972).

18. W. L. Server, Impact Three-Point Bend Testing for Notched and Precracked Specimens, Jn. Testing and Evaluation, 6, 29 (1978).

19. V. Arp, J. H. Wilson, L. Winrich and P. Sikora, Thermal Expansion of Some Engineering Materials from 20 to 293K, Cryogenics, 2, 230 (1962).

20. A. F. Hoenie and D. B. Roach, New Developments in High-Strength Stainless Steels, U. S. Air Force Report DMIC-223, 1966.

21. J. B. Fieldhouse and J. I. Lang, Measurement of Thermal Properties, U. S. Air Force Report WADD-TR-60-904, 1961.

22. C. L. Deel and H. Mindlin, Engineering Data on New Aerospace Structural Materials, AFML-TR-72-196, Vol. 1, Battelle Columbus Labs, September 1972.

23. Anon, Armco 17-4 PH Precipitation-Hardening Stainless Steel Bar and Wire, Armco Steel Corp., S-6C, LA 10273, January, 1974.

24. E. G. Takacs, Armco 17-4 PH, Type 410 - Young's Modulus and Poisson's Ratio, Adv. Mat'ls Div., Armco Steel Corp., October 1976.

25. W. J. Lanning, Torsion Properties of 17-4 PH and 15-5 PH Stainless Steel Bars, Advanced Mat'ls Div., Armco Steel Corp., March 1972.

26. J. F. Knott, Mechanics and Mechanism of Large-Scale Brittle Fracture in Structural Metals, Mat. Sci. Eng., 7, 1 (1971).

27. H. J. Rack, Unpublished Research, Sandia Laboratories, Albuquerque, NM, 87185, April 1975.

28. S. Floreen The Fracture Toughness of Cast High-Strength Steels, Jn. Eng. Mat. Tech., 99, 70 (1977).

This Page Intentionally Left Blank.

APPENDIX A

Mechanical Property Sample Configurations*

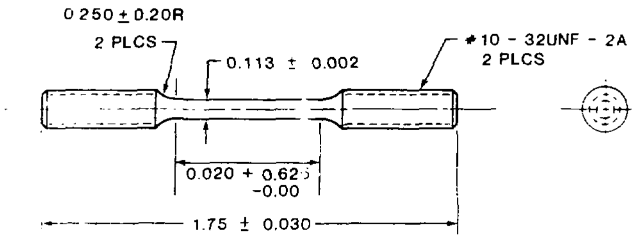

Figure A-1. Subsized Tensile Specimen.

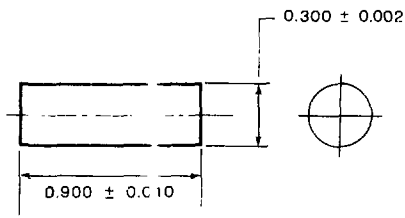

Figure A-2. Cylindrical Compression Specimen.

---

*All dimensions in inches.

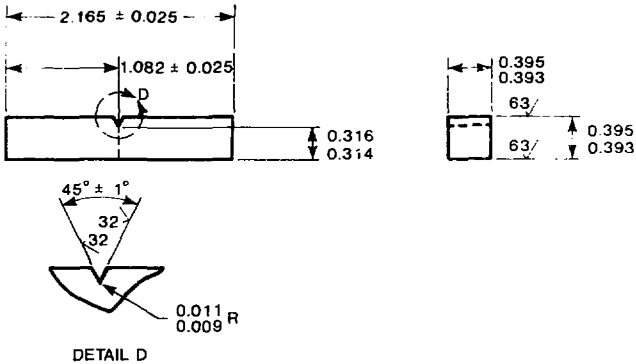

Figure A-3. ASTM Standard Charpy Impact Specimen.

APPENDIX B

Representative Tensile Stress-Strain Curves for Overaged 17-4 PH Stainless Steel Casting

Figure	*Test Temperature (K)*	*Strain Rate (s^{-1})*
B-A	233	1.6×10^{-4}
B-B	233	1.2
B-C	297	1.6×10^{-4}
B-D	297	1.2
B-E	433	1.6×10^{-4}
B-F	433	1.2

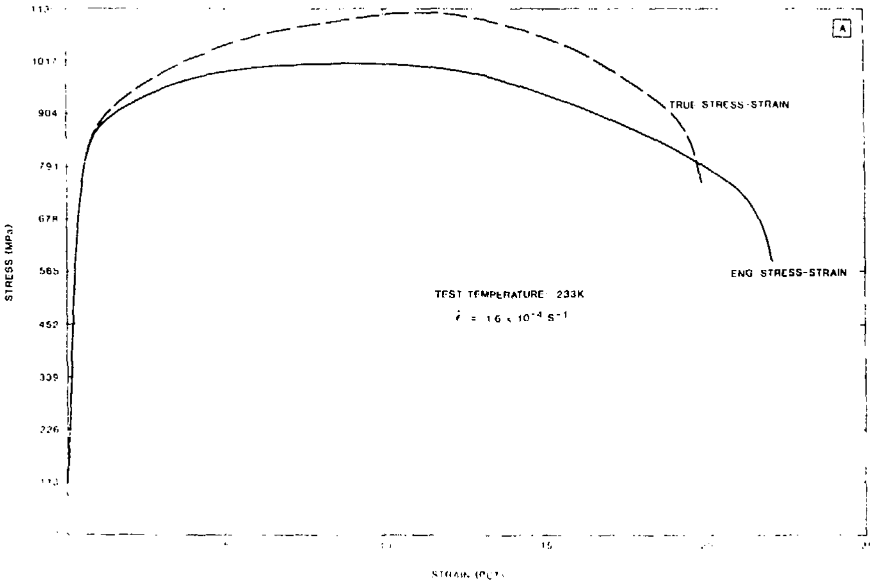
A
1017
904
791
678
565
452
339
226
STRESS (MPa)
TRUE STRESS-STRAIN
ENG STRESS-STRAIN
TEST TEMPERATURE 233K
15

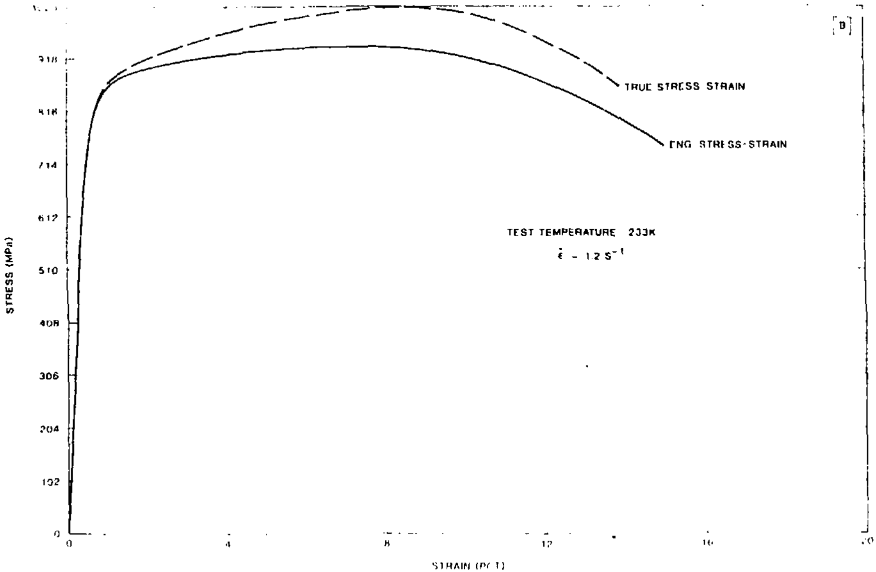

TRUE STRESS STRAIN
ENG STRESS-STRAIN
TEST TEMPERATURE 233K
$\dot{\epsilon}$ = 1.2 S^{-1}
STRESS (MPa)
STRAIN (PCT)
918
816
714
612
510
408
306
204
102
0
0
4
8
12
16
20

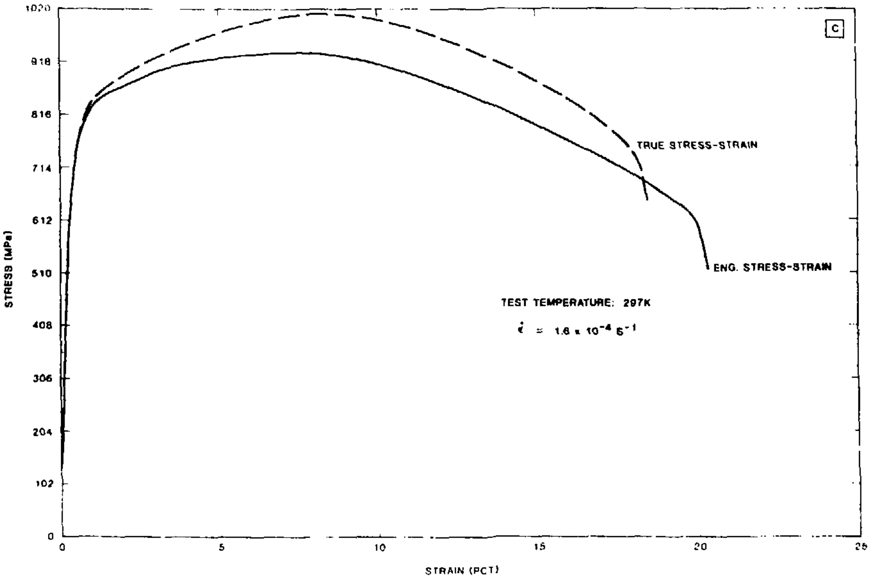

C
TRUE STRESS-STRAIN
ENG. STRESS-STRAIN
TEST TEMPERATURE: 297K
$\dot{\epsilon}$ = 1.6 x 10^{-4} S^{-1}
STRESS (MPa)
0
102
204
306
408
510
612
714
816
918
1020
STRAIN (PCT)
0
5
10
15
20
25

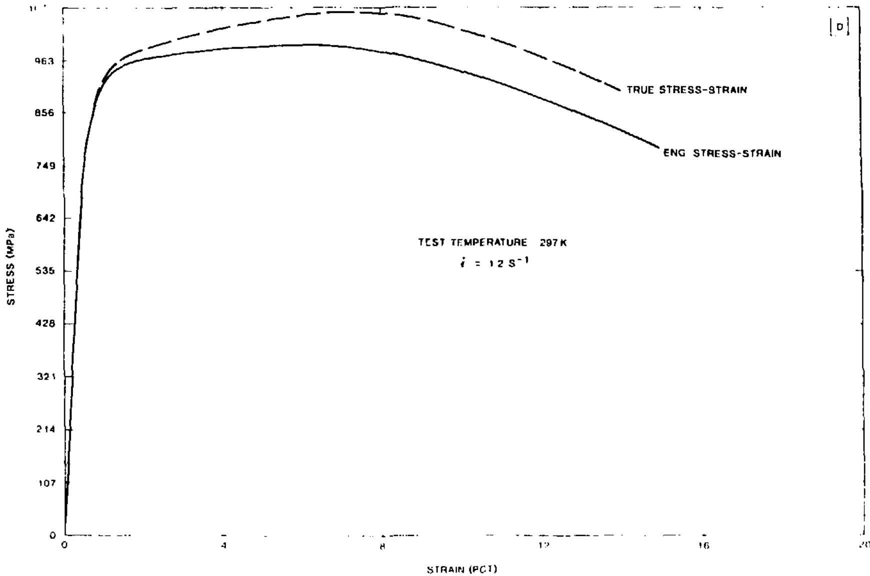
D
963
856
749
642
535
428
321
214
107
0
STRESS (MPa)
0
4
8
12
16
20
STRAIN (PCT)
TRUE STRESS-STRAIN
ENG STRESS-STRAIN
TEST TEMPERATURE 297 K
$\dot{\varepsilon}$ = 1 2 S^{-1}

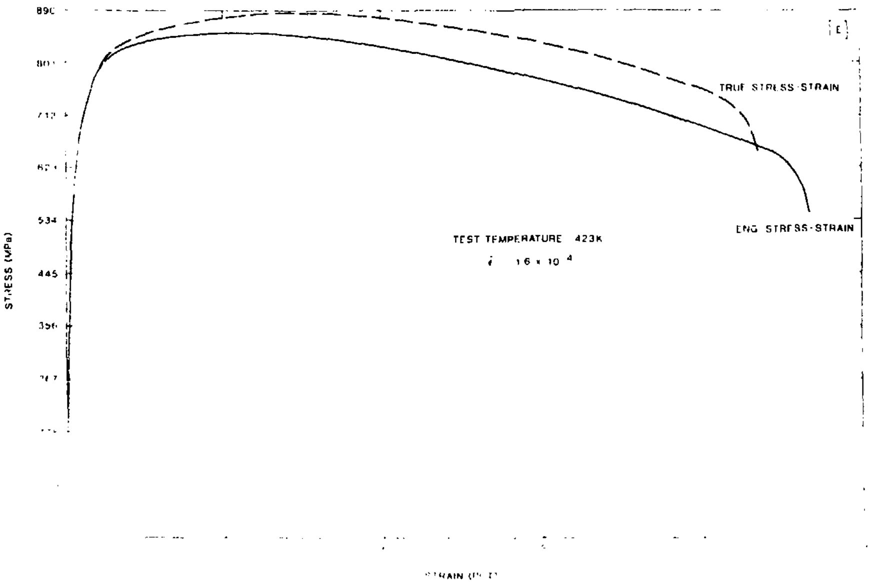
890
801
712
623
534
445
356
267
STRESS (MPa)
TRUE STRESS-STRAIN
ENG STRESS-STRAIN
TEST TEMPERATURE 423K
1.6 x 10 -4
STRAIN

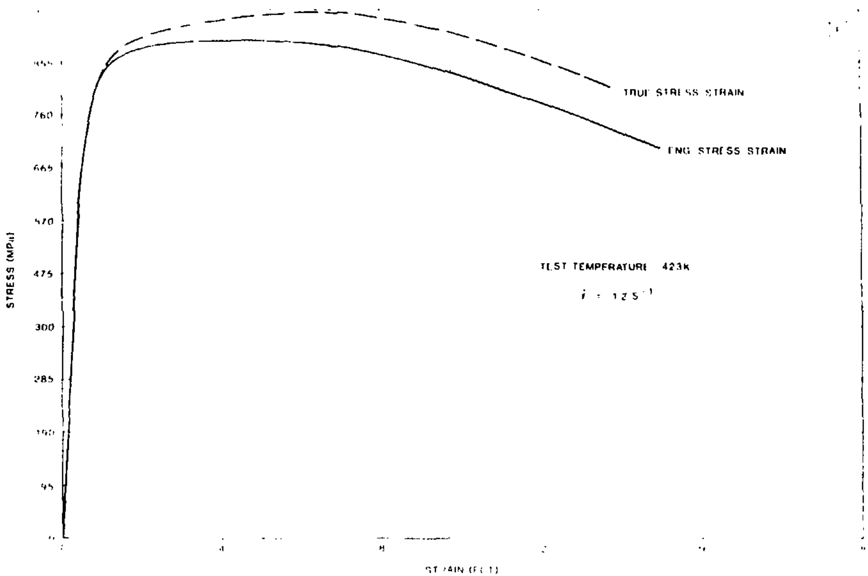
760
665
475
300
285
95
STRESS (MPa)
TRUE STRESS STRAIN
ENG STRESS STRAIN
TEST TEMPERATURE 423K

This Page Intentionally Left Blank.

[illegible]

[illegible] Compressive Stress-Strain [illegible] for [illegible] 17-4 PH Stainless Steel [illegible]

[illegible]	Test Temperature (F)	Strain Rate (s^{-1})
[illegible]	2[illegible]	[illegible] $\times 10^{-4}$
[illegible]	2[illegible]	[illegible]
[illegible]	2[illegible]	[illegible] $\times 10^{[illegible]}$
[illegible]	2[illegible]	[illegible]
[illegible]	4[illegible]	[illegible] $\times 10^{-[illegible]}$
[illegible]	4[illegible]	[illegible]

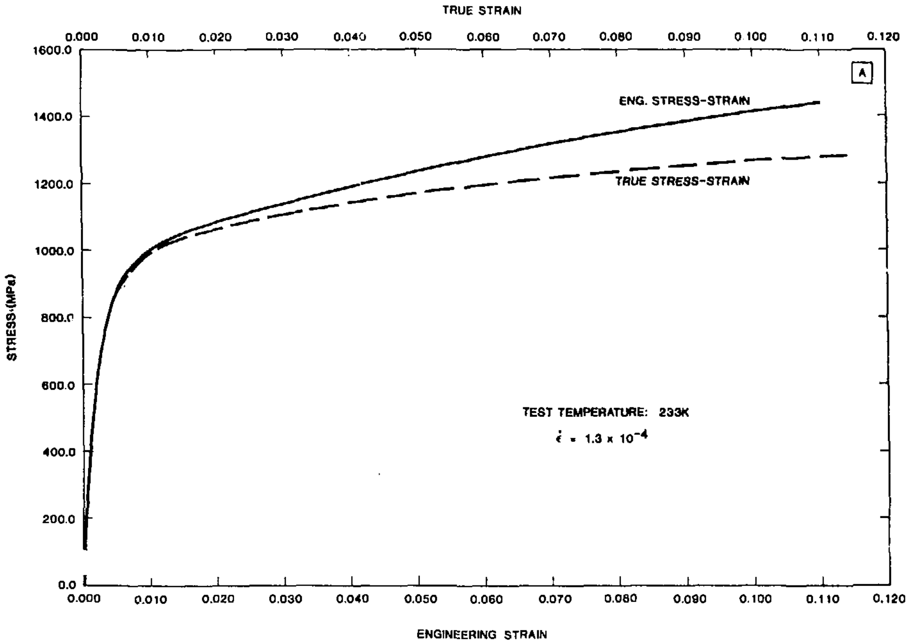

TRUE STRAIN
0.000
0.010
0.020
0.030
0.040
0.050
0.060
0.070
0.080
0.090
0.100
0.110
0.120
A
ENG. STRESS-STRAIN
TRUE STRESS-STRAIN
1600.0
1400.0
1200.0
1000.0
800.0
600.0
400.0
200.0
0.0
STRESS (MPa)
TEST TEMPERATURE: 233K
$\dot{\epsilon}$ = 1.3 x 10^{-4}
0.000
0.010
0.020
0.030
0.040
0.050
0.060
0.070
0.080
0.090
0.100
0.110
0.120
ENGINEERING STRAIN

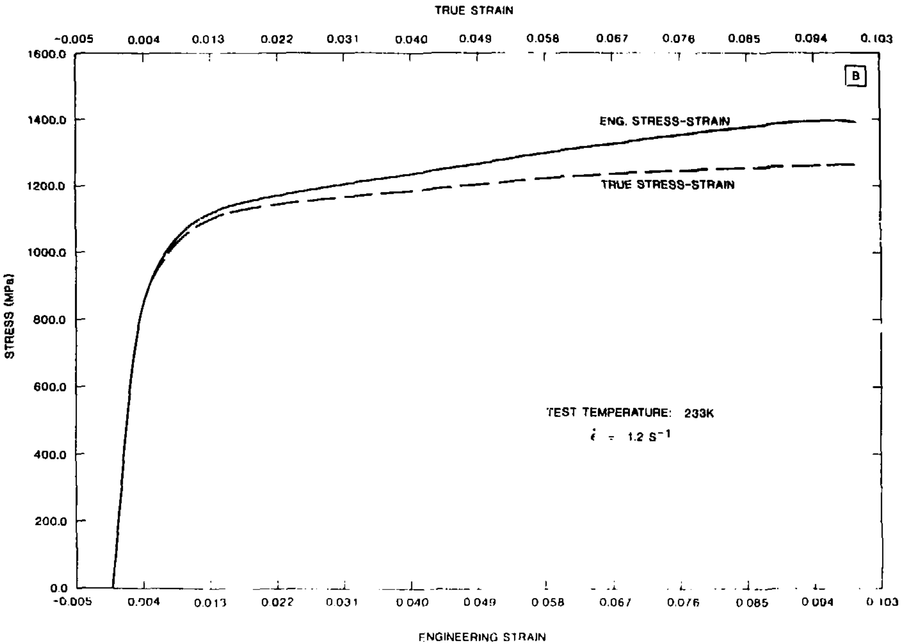
TRUE STRAIN
-0.005
0.004
0.013
0.022
0.031
0.040
0.049
0.058
0.067
0.076
0.085
0.094
0.103
B
ENG. STRESS-STRAIN
TRUE STRESS-STRAIN
TEST TEMPERATURE: 233K
$\dot{\epsilon}$ = 1.2 S^{-1}
STRESS (MPa)
1600.0
1400.0
1200.0
1000.0
800.0
600.0
400.0
200.0
0.0
ENGINEERING STRAIN

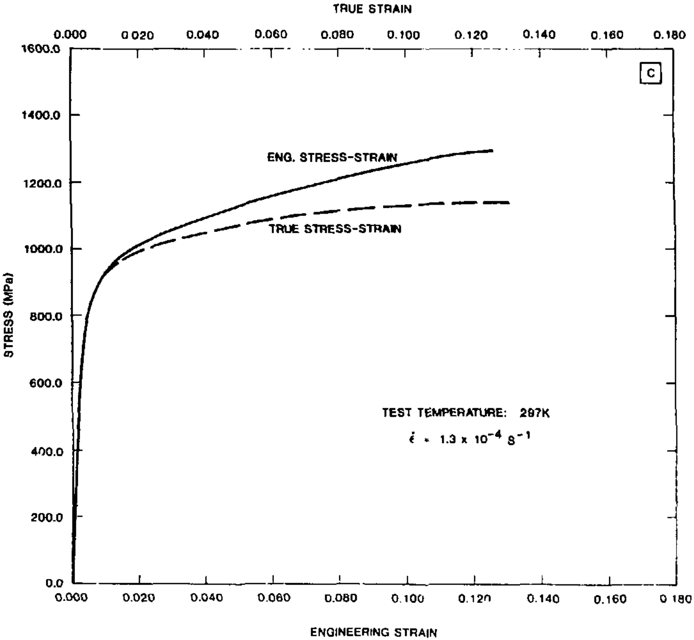

TRUE STRAIN
0.000
0.020
0.040
0.060
0.080
0.100
0.120
0.140
0.160
0.180
1600.0
1400.0
1200.0
1000.0
800.0
600.0
400.0
200.0
0.0
STRESS (MPa)
C
ENG. STRESS-STRAIN
TRUE STRESS-STRAIN
TEST TEMPERATURE: 297K
$\dot{\epsilon}$ = 1.3 x 10^{-4} S^{-1}
0.000
0.020
0.040
0.060
0.080
0.100
0.120
0.140
0.160
0.180
ENGINEERING STRAIN

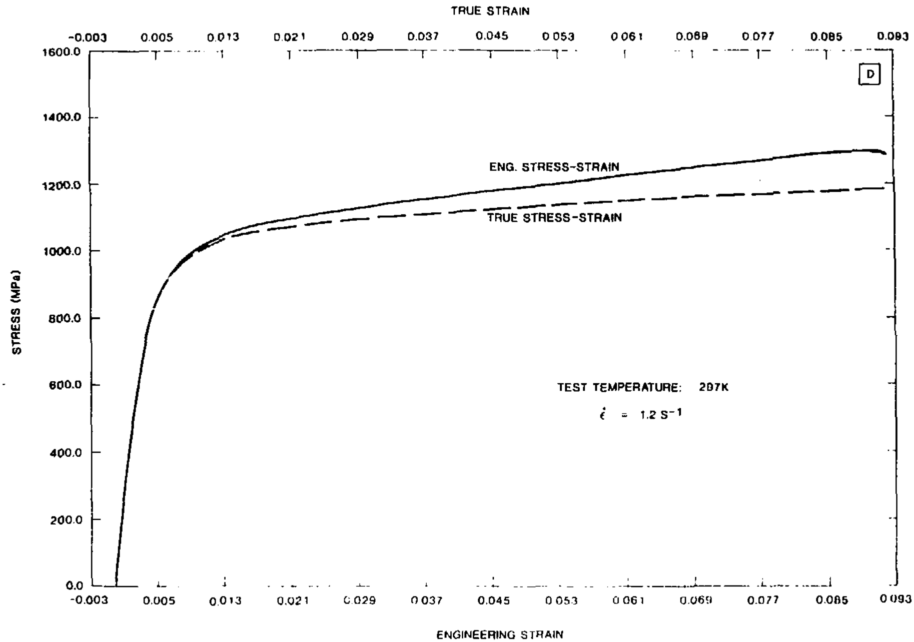
TRUE STRAIN
-0.003
0.005
0.013
0.021
0.029
0.037
0.045
0.053
0.061
0.069
0.077
0.085
0.093
D
STRESS (MPa)
1600.0
1400.0
1200.0
1000.0
800.0
600.0
400.0
200.0
0.0
ENG. STRESS-STRAIN
TRUE STRESS-STRAIN
TEST TEMPERATURE: 297K
$\dot{\epsilon}$ = 1.2 S^{-1}
ENGINEERING STRAIN

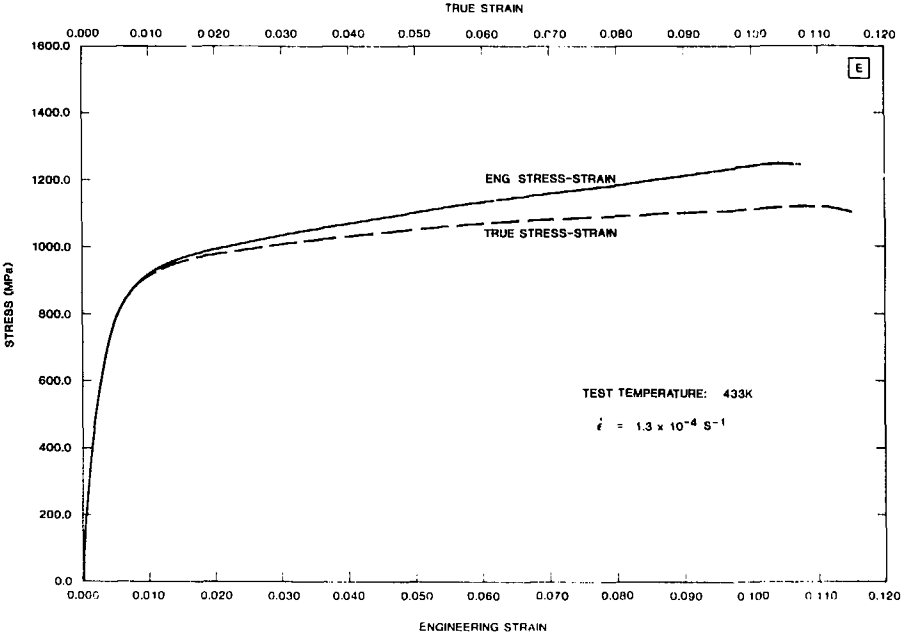
TRUE STRAIN
0.000
0.010
0.020
0.030
0.040
0.050
0.060
0.070
0.080
0.090
0.100
0.110
0.120
E
1600.0
1400.0
1200.0
1000.0
800.0
600.0
400.0
200.0
0.0
STRESS (MPa)
ENG STRESS-STRAIN
TRUE STRESS-STRAIN
TEST TEMPERATURE: 433K
$\dot{\epsilon}$ = 1.3 x 10^{-4} S^{-1}
ENGINEERING STRAIN

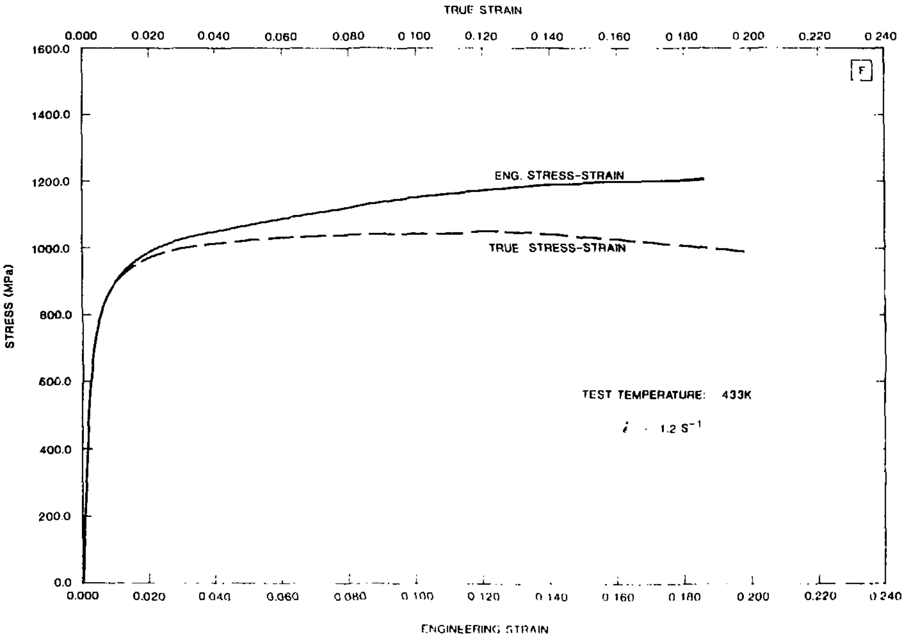
TRUE STRAIN
0.000 0.020 0.040 0.060 0.080 0.100 0.120 0.140 0.160 0.180 0.200 0.220 0.240
F
STRESS (MPa)
1600.0
1400.0
1200.0
1000.0
800.0
600.0
400.0
200.0
0.0
ENG. STRESS-STRAIN
TRUE STRESS-STRAIN
TEST TEMPERATURE: 433K
ε̇ = 1.2 S^-1
0.000 0.020 0.040 0.060 0.080 0.100 0.120 0.140 0.160 0.180 0.200 0.220 0.240
ENGINEERING STRAIN